$$f = (3/8)C_D(v_1 - v_2)|v_1 - v_2|\rho_1\rho_2/(\rho_{22}a),$$
$$q = (3/2)\,\mathrm{Nu}\,k(T_1 - T_2)/(\rho_{22}a^2),$$

where $C_D$ is the drag coefficient; Nu is the Nusselt number; k is the thermal conductivity of the gas; a is the particle radius; and $\rho_{22}$ is the density of the particle material.

Figure 5 shows the parameters of the two-phase mixture to the right of the contact discontinuity, which is found by perturbation theory [6] for $\nu = 1$ and $2\rho_{22}a^2/(9\mu) = 0.01$, where $\mu$ is the gas viscosity.

## LITERATURE CITED


1. S. S. Grigoryan, T. V. Marchenko, and Yu. L. Yakimov, "Transient motions of gas in shock tubes of variable cross section," Prikl. Mekh. Tekh. Fiz., No. 4 (1961).
2. V. P. Korobeinikov, V. V. Markov, and I. S. Men'shov, "Problem of a strong explosion in a dust-filled gas," Transactions of the V. A. Steklov Mathematics Institute [in Russian], Vol. 163 (1984).
3. L. I. Sedov, Similarity and Dimensional Methods in Mechanics [in Russian], Nauka (1987).
4. L. V. Shidlovskaya, "Motion of gas in shock tubes of variable cross section and its application to solar wind perturbations," Izv. Akad. Nauk SSSR, Mekh. Zhidk. Gaza, No. 3 (1976).
5. N. S. Zakharov and V. P. Korobeinikov, "Self-similar motion of gas during the local admission of mass and energy to a combustible mixture," Izv. Akad. Nauk SSSR, Mekh. Zhidk. Gaza, No. 4 (1979).
6. V. P. Korobeinikov, "Perturbation method in flows of dust-filled gas," Usp. Mat. Nauk, 40, No. 4(24), (1985).


# MODELING TRANSIENT TURBULENT AXISYMMETRIC FLOW IN NARROW GAPS BETWEEN CONTOURED ROTATING SURFACES


V. K. Nikul'chikov, N. D. Sosnovskii, and A. V. Shvab



UDC 532.517.4


Rotating channels of various shapes are widely used in modern power plants, turbines, and chemical manufacturing equipment. In particular, efficient air-centrifuge classifiers, which are used in the powder technology, and the express analyzers which are based on them [1, 2] make it possible to fractionate powdered materials by particle dimension at a high rate and to determine their granulometric composition. The working zone of these devices is a narrow gap between rotating contoured surfaces, in which the parts flow and are separated by size by resistive and centrifugal forces. A diagram of the separation zone is presented in Fig. 1.

Here the torsional turbulent flow of an incompressible gas is studied, based on the parabolic equations, obtained from the "narrow channel" approximation. The unsymmetric channel is studied when one of the limiting surfaces is flat and perpendicular to the axis of rotation, and the second is contoured such that the gap width varies according to H = H(R), where R is the radius. The transient nature of the flow is caused by the forced change of the rotation rate of the walls $\Omega$ or the flow Q through the gap. The problem has been examined in the steady-state formulation [3] based on the two-parameter Launder–Jones model [4, 5].

The operational efficiency of these devices can be further enhanced by establishing their fundamental physical characteristics, which are based on models which adequately describe the hydrodynamics of transient torsional axisymmetric flows which are directed both toward the axis of rotation ($Q < 0$, Fig. 1) and toward the periphery ($Q > 0$).


Tomsk. Translated from Prikladnaya Mekhanika i Tekhnicheskaya Fizika, No. 2, pp. 94-101, March-April, 1992. Original article submitted March 6, 1990; revision submitted February 18, 1991.



0021-8944/92/3302-0235$12.50

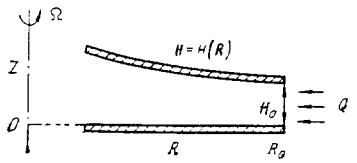


Fig. 1

1. In order to make the equations of motion of the fluid in the gap dimensionless, the radial scale is taken as the input radius $R_0$, and the axial scale is taken as the input gap width $H_0$, and the period $T_0$ for changing Ω or Q is taken as the scale for the time T. The velocity scale is taken as the quantity

$$U_0 = \frac{1}{T_0 H_0}\left|\int_0^{T_0}\int_0^{H_0} U(R_0, Z, T)\,dZ\,dT\right|,$$

where $U(R_0, Z, T)$ is the radial velocity component at the input to the gap.

The Launder–Jones model for transport of the kinetic energy of pulsations K and the dissipation rate for the turbulence energy E is used in order to close the averaged Reynolds equations [4]. The scale for K is taken as

$$K_0 = \frac{1}{T_0 H_0}\int_0^{T_0}\int_0^{H_0} K(R_0, Z, T)\,dZ\,dT.$$

The scale for the dissipation of the turbulence energy can be related to the scale for the kinetic pulsation energy through the A. N. Kolmogorov relation $E_0 = c_d K_0^{3/2}/L_0$, where $L_0$ is the linear turbulence scale at the input, and the constant $c_d \approx 0.1$ [6].

The equations for turbulent transient axisymmetric motion of a fluid in cylindrical coordinates are written under the assumption that the relative width of the channel $\beta = H_0/R_0$ is small. This assumption made it possible to estimate the order of magnitude of the specific terms in the system of Reynolds equations and to throw out some of the terms, in analogy to the classical method of obtaining the boundary layer equations. Thus, of the viscous terms, the term with the second derivative in the axial coordinate has the largest order; by comparison the others are of order $\beta^2$. The derivatives of the turbulent Reynolds stresses remain only with respect to the axial coordinate. Then, considering the Boussinesq formula, the dimensional equation for momentum transport in the radial direction, for example, has the form

$$\mathrm{Sh}\frac{\partial u}{\partial t} + u\frac{\partial u}{\partial r} + \frac{w}{\beta}\frac{\partial u}{\partial z} - \frac{v^2}{r} + \frac{\partial p}{\partial r} = \frac{1}{\beta\,\mathrm{Re}}\frac{\partial}{\partial z}\left[(1+\nu_t)\frac{\partial u}{\partial z}\right].$$

The equations for the rotational velocity component, the transport of the kinetic energy for turbulent pulsation, and the dissipation rate of the turbulence energy are transformed in the same way. Instead of the equation for the axial component, we obtain the standard condition $\partial p/\partial z = 0$.

In order to simplify the numerical integration of the equations, the axial coordinate $z = Z/H_0$ should be replaced by $z = \xi h(r)$, which reduces the region with the curvilinear boundary to a plane-parallel channel where $h = h(r) = H(R)/H_0$ is the dimensionless equation of the profile of the limiting surface. In order to do the calculations on a uniform grid, a new coordinate s is introduced, which is related to ξ by the relationship $\xi = g(s)$, where g(s) is a specially selected function, for which a constant step in s corresponds to a decreasing step in ξ at the wall. After a double transformation of coordinates, the equations for fluid flow, continuity, and the k–ε turbulence model are obtained in final form:

$$\mathrm{Sh}\frac{\partial u}{\partial t} + u\frac{\partial u}{\partial r} - \left(u\frac{gh'}{g'h} - \frac{w}{\beta g' h}\right)\frac{\partial u}{\partial s} - \frac{v^2}{r} + \frac{\partial p}{\partial r} = \frac{1}{\beta g' h^2 \mathrm{Re}}\frac{\partial}{\partial s}\left(\frac{1+\nu_t}{g'}\frac{\partial u}{\partial s}\right); \qquad (1.1)$$

$$\mathrm{Sh}\frac{\partial v}{\partial t}+u\frac{\partial v}{\partial r}-\left(u\frac{gh'}{g'h}-\frac{w}{\beta g'h}\right)\frac{\partial v}{\partial s}+\frac{uv}{r}=\frac{1}{\beta g'h^2\mathrm{Re}}\frac{\partial}{\partial s}\left(\frac{1+\nu_t}{g'}\frac{\partial v}{\partial s}\right); \tag{1.2}$$

$$\frac{1}{r}\frac{\partial(ru)}{\partial r}-\frac{gh'}{g'h}\frac{\partial u}{\partial s}+\frac{1}{\beta g'h}\frac{\partial w}{\partial s}=0; \tag{1.3}$$

$$\mathrm{Sh}\frac{\partial k}{\partial t}+u\frac{\partial k}{\partial r}-\left(u\frac{gh'}{g'h}-\frac{w}{\beta g'h}\right)\frac{\partial k}{\partial s}=\frac{1}{\beta g'h^2\mathrm{Re}}\frac{\partial}{\partial s}\left(\frac{1+\nu_t}{g'}\frac{\partial k}{\partial s}\right)+ \tag{1.4}$$

$$+\frac{\nu_t}{\beta g'^2h^2\mathrm{ReTu}^2}\left[\left(\frac{\partial u}{\partial s}\right)^2+\left(\frac{\partial v}{\partial s}\right)^2\right]+\frac{\mathrm{DiTu}}{\beta}\varepsilon-\frac{2}{\beta g'^2h^2\mathrm{Re}}\left(\frac{\partial k^{1/2}}{\partial s}\right)^2;$$

$$\mathrm{Sh}\frac{\partial \varepsilon}{\partial t}+u\frac{\partial \varepsilon}{\partial r}-\left(u\frac{gh'}{g'h}-\frac{w}{\beta g'h}\right)\frac{\partial \varepsilon}{\partial s}=\frac{1}{\beta g'h^2\mathrm{Re}}\frac{\partial}{\partial s}\left(\frac{\sigma+\nu_t}{\sigma g'}\frac{\partial \varepsilon}{\partial s}\right)+ \tag{1.5}$$

$$+\frac{c_{\varepsilon 1}\nu_t}{\beta g'^2h^2\mathrm{ReTu}^2}\left[\left(\frac{\partial u}{\partial s}\right)^2+\left(\frac{\partial v}{\partial s}\right)^2\right]\frac{\varepsilon}{k}-\frac{c_{\varepsilon 2}\mathrm{DiTu}}{\beta}\frac{\varepsilon^2}{k}+$$

$$+\frac{2\nu_t}{\beta g'^2h^4\mathrm{Re}^2\mathrm{DiTu}^3}\left\{\frac{\partial}{\partial s}\left[\frac{1}{g'^2}\left(\frac{\partial u}{\partial s}\right)^2+\frac{1}{g'^2}\left(\frac{\partial v}{\partial s}\right)^2\right]^{1/2}\right\}^2.$$

The dimensionless variables and unknown functions in (1.1)-(1.5) are reduced by the ratios: $t = T/T_0$, $r = R/R_0$, $u = U/U_0$, $v = V/U_0$, $w = W/U_0$, $p = P/\rho U_0^2$, $\nu_t = \nu_T/\nu$, $k = K/K_0$, and $\varepsilon = E/E_0$. Here Z is the axial coordinate: U, V, and W are the radial, rotational, and axial components of the fluid velocity; P is the pressure; $\nu$ and $\nu_T$ are the coefficients of molecular and turbulent viscosity; $g' = dg/ds$; and $h' = dh/dr$.

The model constants and the function for the relative coefficient of turbulent viscosity are chosen according to [5]: $\nu_t = c_\mu \mathrm{Re}_k$, where $c_\mu = 0.09\cdot\exp[-3.4/(1 + 0.02\ \mathrm{Re}_k)^2]$; $\mathrm{Re}_k = \mathrm{Re}\cdot\mathrm{Tu}\cdot k^2/(\mathrm{Di}\cdot\varepsilon)$; $c_{\varepsilon 1} = 1.44$; $c_{\varepsilon 2} = 1.92\cdot[1 - 0.3\cdot\exp(-\mathrm{Re}_k^2)]$; and $\sigma = 1.3$.

The boundary conditions are given by the initial and input distribution of the velocity components and the turbulence characteristics, the adhesion of the fluid to the rotating surfaces, the impermeability of the surfaces, and the degeneration of turbulence at the walls:

$$t = 0\colon u, v, k, \varepsilon(r, s, t) = u_{\text{н}}, v_{\text{н}}, k_{\text{н}}, \varepsilon_{\text{н}}(r, s); \tag{1.6}$$

$$r = 1\colon u, v, k, \varepsilon(r, s, t) = u_{\text{в}}, v_{\text{в}}, k_{\text{в}}, \varepsilon_{\text{в}}(s, t); \tag{1.7}$$

$$s = 0, s = 1\colon u, w, k, \varepsilon(r, s, t) = 0, v(r, s, t) = \mathrm{Ro}^{-1}r\omega(t). \tag{1.8}$$

Because the axial component is found from the first-order continuity equation, one of the impermeability conditions (1.8) for w is redundant. It can be used to determine the pressure gradient. However, it is more convenient to calculate $\partial p/\partial r$ from the flow conservation equation, which results from this condition. Therefore, one of the boundary conditions (1.8) for w is replaced by an integral equation for conserving the flow over the radius

$$rh\int_0^1 g'uds = q(t). \tag{1.9}$$

Here $\omega = \Omega/\Omega_0$; $\Omega_0 = \frac{1}{T_0}\int_0^{T_0}\Omega dT$; $q = Q/Q_0$; $Q_0 = \frac{1}{T_0}\left|\int_0^{T_0} QdT\right|$. We also note that the input distribution of the rotational velocity (1.7) can be represented as

$$v_{\text{в}}(s, t) = \frac{V_{\text{в}}}{U_0} = \frac{V_0}{U_0}\frac{V_{\text{в}}}{V_0} = \mathrm{Ro}_{\text{f}}^{-1}\bar{v}_{\text{в}}(s, t).$$

Here

$$\bar{v}_{\text{в}}(s, t) = V_{\text{в}}/V_0;\ V_{\text{в}} = V(R_0, Z, T);\ V_0 = \frac{1}{T_0H_0}\int_0^{T_0}\int_0^{H_0} V_{\text{в}}dZdT.$$

Thus, the transient flow in contoured rotation channels is characterized by the following similarity criteria, which follow from Eqs. (1.1)-(1.5) and the boundary conditions (1.6)-(1.9): $\mathrm{Sh} = R_0/U_0T_0$ is the Strouhal number; $\mathrm{Re} = U_0H_0/\nu$ is the Reynolds number; $\mathrm{Ro} = U_0/\Omega_0R_0$ and $\mathrm{Ro}_{\text{f}} = U_0/V_0$ are the Rossby numbers, which represent the degree of torsion of the

solid boundaries and the fluid, respectively; and $\beta$ and $h = h(r)$ are the geometric criteria. The turbulence is characterized by the criteria $Tu = \sqrt{K_0}/U_0$ and $Di = c_d H_0/L_0$.

2. The transient equations of the averaged motion and the k–ε model of turbulence are nonlinear parabolic equations, which can be represented in the general form

$$\mathrm{Sh}\,\frac{\partial f}{\partial t} + a\frac{\partial f}{\partial r} + b\frac{\partial f}{\partial s} = c\,\frac{\partial}{\partial s}\left(d\,\frac{\partial f}{\partial s}\right) + e, \tag{2.1}$$

where the coefficients a, b, c, d, and e depend on the coordinates, time, and the unknown functions f. The system of equations is solved by using a two-layer implicit difference method [7] for a second-order approximation in s and a first-order approximation in r and t, which for Eq. (2.1) has the form

$$\mathrm{Sh}\,\frac{f_{i,j+1}^{m+1} - f_{i,j+1}^{m}}{\Delta t} + a_{i,j+1}^{m+1}\frac{f_{i,j+1}^{m+1} - f_{i,j}^{m+1}}{\Delta r} + b_{i,j+1}^{m+1}\frac{f_{i+1,j+1}^{m+1} - f_{i-1,j+1}^{m+1}}{2\Delta S} =$$
$$= c_{i,j+1}\frac{d_{i+1/2,j+1}^{m+1}\left(f_{i+1,j+1}^{m+1} - f_{i,j+1}^{m+1}\right) - d_{i-1/2,j+1}^{m+1}\left(f_{i,j+1}^{m+1} - f_{i-1,j+1}^{m+1}\right)}{\Delta s^2} + e_{i,j+1}^{m+1}. \tag{2.2}$$

Here $\Delta t$, $\Delta r$, and $\Delta s$ are the steps in time and along the radial and transverse coordinates, and the indices m, i, and j correspond to the directions t, s, and r.

The continuity equation (1.3) is approximated in the form

$$\frac{r_{j+1}\left(u_{i+1,j+1}^{m+1} + u_{i,j+1}^{m+1}\right) - r_j\left(u_{i+1,j}^{m+1} + u_{i,j}^{m+1}\right)}{2r_{j+1}\Delta r} - \frac{g_{i+1/2}\,h_{j+1}'}{g_{i+1/2}'\,h_{j+1}}\,\frac{u_{i+1,j+1}^{m+1} - u_{i,j+1}^{m+1}}{\Delta s} +$$
$$+ \frac{1}{\beta g_{i+1/2}'\,h_{j+1}}\,\frac{w_{i+1,j+1}^{m+1} - w_{i,j+1}^{m+1}}{\Delta s} = 0. \tag{2.3}$$

The system of difference equations (2.2) and (2.3) with difference analogs of the boundary conditions (1.6)-(1.9) is solved as follows. Initially, in the "piecewise stationary" method, conditions are held fixed to find the stationary field of the velocity and the turbulence characteristics, which corresponds to the initial condition (1.6). Then the solution is iterated on the (m + 1)-th layer in time using a trial-and-error method on the transverse coordinate s. The resultant distribution is compared with the previous one on the m-th layer. If their difference exceeds a previously specified small number, even at one point in space, the values of the unknown functions at the (m + 1)-th layer are assumed the m-th layer, after which the iteration is repeated again, until the convergence criteria are satisfied at all points. The resultant stationary field for the initial values of the flow parameters serve as the initial condition for the transient problem. It is solved by the same method of (2.2) and (2.3); however the convergence of the iterations is verified, not between the (m + 1)-th and m-th layers in time, but between the preceding and following iterations on the (j + 1)-th layer along the radius of the (m + 1)-th layer in time. When the iteration convergence criteria are satisfied for all values j on the (m + 1)-th layer, we go on to calculate the unknown quantities at the following moment of time.

The pressure gradient $\partial p/\partial r$, which enters Eq. (1.1), is determined from the integral condition (1.9) for conversing flow along the radius, which uses the method detailed in [7]. Its essence is that the solution of the difference equation for $u_{i,j+1}^{m+1}$ can be written as $u_{i,j+1}^{m+1} = \overset{\circ}{u}_{i,j+1}^{m+1} + \tilde{u}_{i,j+1}^{m+1}(-\partial p/\partial r)_{j+1}^{m+1}$ in view of its linearity, where $\overset{\circ}{u}_{i,j+1}^{m+1}$ is the solution which formally satisfies $\partial p/\partial r = 0$ and $\tilde{u}_{i,j+1}^{m+1}$ is the solution of the difference equation with the right side equal to unity.

3. The solution method and the possibility of applying the k–ε model to this type of flow was verified by using a test calculation in a plane-parallel channel $h(r) = 1$ for the flow parameters in [8] with stationary fluid flow from the rotation axis to the periphery. The lack of experimental data in the literature made it impossible to test transient flow. However, the agreement of velocity fields computed with the stationary equations [3] and with the piecewise stationary method is practical evidence that the method is also correct for solving a transient problem. Due to symmetry, the calculation was done for the half height of a plane-parallel channel with 51 nodes in the grid for the transverse coordinate

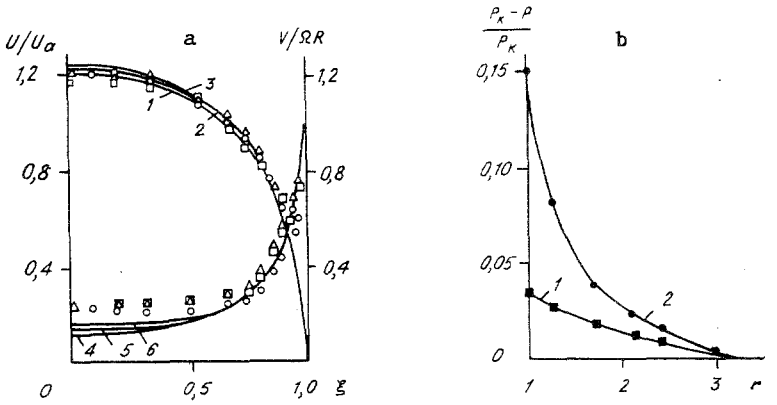


Fig. 2

and an axial scale of $H_0/2$. The function which controls the density of the grid had the form $g(s) = \sin \pi s/2$. The zone width for the last zone at the wall was $\Delta\xi \approx 4 \cdot 10^{-4}$, which guaranteed at least 10 points in the viscous sublayer.

The rotational and radial velocity components and the pressure are compared with experimental data [8] in Fig. 2. As with the authors' experiments, it was found that the distributions of the radial component, ratioed to the average flow velocity $U_a = Q/2\pi RH$, and the rotational component, ratioed to the local linear velocity at the boundaries $\Omega R$, were close to similar ones in Fig. 2a for identical parameters $Re_1 = Re/r$ and $Re_2 = r \cdot Re/Ro$ ($Re_1 = 1602$; $Re_2 = 3265$; Ro Tu = 0.1; Di = 2; $\beta = 0.085$; curves 1 and 4 and the circles correspond to a radius r = 1.71; 2 and 5 and the triangles to r = 2.43; and 3 and 6 and the squares to r = 2.71). Calculated values agree well with experimental points [8] in Fig. 2b ($\beta = 0.057$; Di = 2; for curve 1: Re = 1780, Ro = 1.37, Tu = 0.07; 2: Re = 3990, Ro = 3.07, and Tu = 0.03).

The satisfactory agreement of the calculated and experimental distributions of the fluid velocity components and of the pressure indicates the validity of the k–ε model for examining the class of rotational flows.

4. In conducting numerical calculations of the transient turbulent flow from the periphery to the axis of rotation in contoured channels, a uniform grid was used with 51 nodes in the transverse coordinate and 26 nodes along the radius, including the boundaries. The calculation was done to a radius r = 0.5. The time step was $\Delta t = 0.001$-$0.01$. The system parameters were varied in time, both periodically as $|q| = 1 + A \sin 2\pi t$ ($|A| < 1$ is the amplitude of the oscillations) and linearly increasing or decreasing in time $\omega = B + 2(1 - B)t$ ($0 < B < 2$ is the initial value of the parameter). The velocity components of the fluid and the turbulence characteristics were assumed uniform in the axial coordinate at the entrance to the channel.

Figure 3 shows the velocity components of the fluid at various times for a pulsating flow given by $q = -(1 + 0.5 \sin 2\pi t)$, and a constant rotation rate at the boundary $\omega = 1$. The other parameters are as follows: Re = 1050, Ro = 0.5, $Ro_f = 0.5$, Sh = 12.5, $\beta = 0.1$, Tu = 0.2, and Di = 2. The equation of the channel, which widens toward the axis of rotation, has the form $h = 3 - 2r$. Curves 1-7 in Fig. 3a correspond to the radial velocity component of the fluid at radius r = 0.5 at times 0, 0.2, 0.4, 0.5, 0.6, 0.8, and 1. The profile of the radial velocity component shows the most deformation at minimum values of the flow parameter $|q|$. The asymmetry of the curves appears basically in the region next to the wall, where the velocity peaks higher at the upper contoured surface in most cases than on the lower disk. The effect of the transient flow can be seen by comparing curves 1, 4, and 7 for the same value of the flow q. Curve 1 corresponds to the stationary solution at time t = 0; 4 and 7 to the decaying and growing sections of the sinusoid. The most deformation of the curve of the radial velocity is observed for increasing flow; the least for decaying $|q|$, and the stationary curve lies in the middle. However, the effect of the transience shows up markedly for Sh > 1. At lower Strouhal numbers the velocity curves practically coincide. These regimes can be considered quasistationary. The stationary problem can be solved for them at each required moment in time, which is much simpler.

The distributions of the rotational velocity component at various times for a varying flow differ little from the stationary distributions. They converge to a single curve on

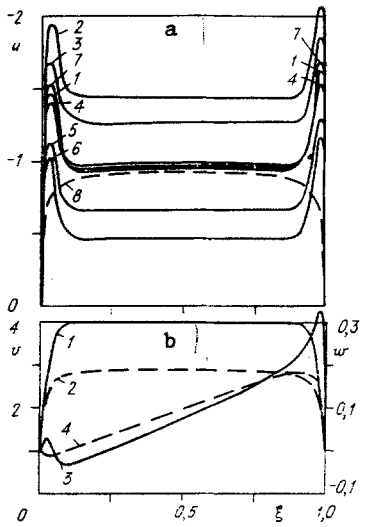


Fig. 3

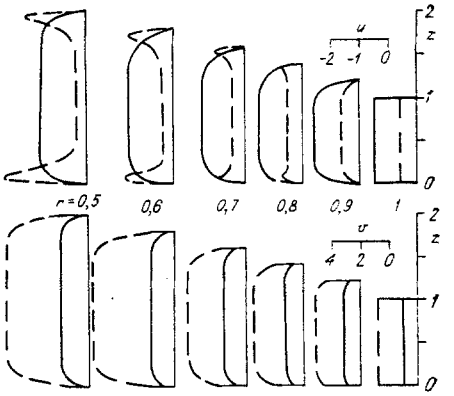


Fig. 4

the graph (Fig. 3b, lines 1 and 2 at r = 0.5 and 0.7). It can be seen that, for a specified uniform velocity profile at the inlet, the uniformity is maintained at the inertial core which occupies a significant fraction of the gap all the way to r = 0.5. The rotational velocity component in the inertial flow core develops along the radius as a vortex–sink combination. Its level has a significant effect on the distribution of the radial velocity component throughout the cross section. Thus, at the mean and initial radii, the profile of the radial velocity component has the usual form (curve 8 at r = 0.7 at t = 0, Fig. 3a). At subsequent radii, a so-called Eckman boundary layer occurs, due to the nonuniform, increasing distribution of the rotational component across the width of the channel. The flow increases in this layer compared to the core and greatly exceeds it at r = 0.5. That is, the deformation of the profile of the radial velocity component increases (for example, curve 1 in Fig. 3a).

The distributions of the axial velocity component at radii r = 0.5 and 0.7 are shown in Fig. 3b (curves 3 and 4, respectively). It can be seen that the velocity of the transverse flow increases near the axis of rotation at the upper contoured surface. The intensity of the turbulence in most cases decreases deep within the channel compared to the initial value or maintains roughly the same value along the radius.

Figure 4 illustrates the development of the curves of the radial and rotational components of the fluid velocity along the radius and in time in a channel which widens toward the axis of rotation as $h = 3 - 2r$ according to the equation $|q| = 1.5 - t$ and $\omega = 0.5 + t$. That is, the fluid flow decreases and the rotation rate of the walls increases. Here Sh = 0.01, and the other physical and geometric parameters are the same as in Fig. 3. The solid curves show the velocity at time t = 0, and the dashed lines at time t = 0.9. From the curves it can be seen that the deformation of the curve of the radial velocity component approaches critical values even at r = 0.5, due to the increase in the centrifugal force with time and the drop in the flow, and then increasing flows start, which cannot be calculated within the framework of the boundary-layer model.

As the investigation has shown, the effect of the criteria Ro and $Ro_f$ on the flow is determined by the interaction of the forces of flow inertia and centrifugal factors. When these criteria grow together while others are fixed, the longitudinal inertia and the profile of the radial component tend to retain their shapes. As they decrease, centrifugal effects increase, and the profile of the radial velocity component undergoes deformation.

## LITERATURE CITED

1. V. A. Shvab, A. T. Roslyak, et al., "Centrifugal classifiers," Inventor's Certificate No. 740,305, USSR, Otkryt. Izobret., No. 22 (1980).
2. V. K. Nikul'chikov, A. A. Kolesnikov, et al., "Device for analyzing the dispersion of powders," Inventor's Certificate No. 1,486,888, USSR, Otkryt. Izobret., No. 22 (1989).

3. N. D. Sosnovski, "Hydrodynamics and the process of separating solid particles in rotating channels with contoured boundaries," Author's Abstract of Candidate Dissertation in the Physical-Mathematical Sciences, Leningrad Polytechnic Institute, Leningrad (1988).
4. W. P. Jones and B. E. Launder, "Prediction of laminarization with a two-equation model of turbulence," Intern. J. Heat Mass Transfer., 15, No. 2 (1972).
5. Launder, Pridden, and Sharma, "Calculation of a turbulent boundary layer on rotating curvilinear surfaces," Trans. Am. Soc. Eng. Mechanics. Theoretical Basis for Engineering Calculations, No. 1 (1977).
6. U. Frost and T. Moulden (eds.), Turbulence, Principles and Applications [Russian translation], Mir, Moscow (1980).
7. L. A. Dorfman, Numerical Methods in the Hydrodynamics of Turbines [in Russian], Énergiya, Leningrad (1974).
8. E. Bakke, J. F. Kreider, and F. Kreith, "Turbulent source flow between parallel stationary and co-rotating disks," J. Fluid Mech., 58, Part 2 (1973).

# SEDIMENTATION OF A CLOUD OF A BIDISPERSED AEROSOL ONTO A FLAT HORIZONTAL SURFACE

G. M. Makhviladze, D. V. Serov, and S. E. Yakush

UDC 532.529

A characteristic feature of the motion of a cloud of monodispersed particles in the open under the influence of gravity is the clear appearance of collective effects, which result from the hydrodynamic interaction of the falling particles through a gaseous carrier. Depending on the degree of this interaction, it is convenient to distinguish two sedimentation regimes [1, 2]. In the entrainment regime, the particles completely or partially entrap the medium between them; as a result, the falling velocity of an aggregate of particles exceeds the velocity of a single particle, and the cloud takes on the shape of a bowl or a torus. In the filtration regime, the particles settle out practically independent of each other, the velocity of the center of mass of the cloud equals the falling velocity of a single particle, and the cloud shape changes extremely slowly. The entrainment regime occurs if there is a large enough concentration of fine particles in the cloud [2]. As the particle dimension increases or their concentration decreases, there is a transition to the filtration regime.

Particles of identical dimensions (monodispersed aerosol) have been examined in theoretical studies [2-5] on the free sedimentation of an aggregate of fine particles under the force of gravity. Actually, real aerosol formations usually consist of particles of various dimensions. The most extensive situation is the one where particles can be separated into two characteristic dimensions (bidispersed aerosol). An example is natural rain clouds, which consist of mist and rain drops.

Here an approach investigate monodispersed aerosols [2] is generalized to the case of a bidispersed cloud. It is shown that as this cloud settles out, it either divides into two independently moving monodispersed clouds or settles as a single one. The conditions are found for which each of these regimes is realized. The dispersion laws of particles on the sedimentation surface are also found.

1. Let a cloud of solid or liquid spherical particles of two types be formed in a quiescent gas above a flat horizontal surface at time $t = 0$. The particles are of the same material and differ only in diameter. They start to move downwards due to the force of gravity and leave the suspending gas behind. The problem is to calculate the transient motion of the particles and the gas until all the particles have settled out on the underlying surface. It is assumed that the dimension of the cloud in one of its horizontal directions is much larger than the other, which makes it possible to seek a solution independent of one of

Moscow. Translated from Prikladnaya Mekhanika i Tekhnicheskaya Fizika, No. 2, pp. 101-108, March-April, 1992. Original article submitted November 20, 1990.

0021-8944/92/3302-0241$12.50  